POSS-Al-porphyrin-imidazolium cross-linked network as catalytic bifunctional platform for the conversion of CO_2 with epoxides.

Anthony Morena,[a,b] Vincenzo Campisciano,[b] Andrea Santiago-Portillo,[a] Michelangelo Gruttadauria,*[b] Francesco Giacalone,*[b] Carmela Aprile*[a]

[a]*Unit of Nanomaterials Chemistry, Department of Chemistry, NISM, University of Namur, 61 rue de Bruxelles, 5000 Namur, Belgium*

[b]*Department of Biological, Chemical and Pharmaceutical Sciences and Technologies (STEBICEF)- University of Palermo and INSTM UdR – Palermo, Viale delle Scienze, Ed.17, Palermo I-90128, Italy*

Abstract:

Two heterogeneous catalysts were prepared with the aim of following the promising path of CO_2 fixation onto epoxides. The synthetic procedure involves a radical copolymerization of an octavinylsilsesquioxane as inorganic core building block and tetrastyrylporphyrin aluminum chloride monomer (TSP_AlCl) in presence (POSS_TSP_AlCl_imiBr) or in absence (POSS_TSP_AlCl) of a bis-vinylimidazolium bromide salt (bis-imiBr), in order to investigate if the bifunctional heterogeneous material can display better catalytic performance than the separate species. All the solids were fully characterized and tested in the synthesis of cyclic carbonates starting from CO_2 and several epoxides. The synergic cooperation of the two co-catalytic species (Lewis acid/imiBr) was observed. POSS_TSP_AlCl_imiBr showed to be a recyclable material with an excellent activity and TON and TOF values up to 16000 and 5000, respectively. These excellent results, even under mild reaction and solvent-free conditions, were attributed to a twofold effect: the proximity between the two active sites due to the direct covalent bond between the porphyrin and the imidazolium component and the increasing local concentration of active sites effect that is obtained by functionalizing the silica cage at all its vertices.

Keywords: Carbon Dioxide conversion; Bifunctional catalyst; Silsesquioxanes; Al-porphyrin; Cyclic Carbonates

1. Introduction:

According to the Intergovernmental Panel on Climate Change (IPCC) of the United Nations reports[1], the increasing amount of CO_2 in the atmosphere should be reduced using carbon capture strategies while decreasing carbon emissions. Carbon dioxide is not only a waste, but it is also a renewable source of carbon, which can be converted into more useful products and is therefore considered as one of the most available, nontoxic, abundant and economical carbon (C1) feedstock [2-4]. For these reasons the attention of researchers from both academia and industry has been focused on the attempt to capture, reuse, and valorize CO_2. Even though the extensive use of carbon dioxide as C1 building block in chemical production cannot solve environmental problems alone, it can efficiently replace other chemicals with a major climate change impact (CII) such as phosgene or chlorofluorocarbons (CFCs)[5, 6]. Despite the above-mentioned advantages, the use of carbon dioxide has a major drawback related to its thermodynamic stability. There are several ways to overcome this problem, and one of the most advantageous is to incorporate the CO_2 molecule into an organic substrate. In this context, the use of high-energy starting molecules such as epoxides with a suitable catalyst enables carbon dioxide to be converted via one of the most interesting routes: the production of cyclic carbonates[7-9]. This family of compounds comprises high-value added chemicals that find common applications as aprotic polar solvents, intermediates for fine or bulk chemical synthesis, and battery electrolytes[10-13]. Moreover, it is important to mention that the production of cyclic carbonates by reaction of carbon dioxide with epoxides is a process that highly satisfies the principles of green chemistry[14, 15]. First of all it uses a renewable resource such as CO_2, displays an atom economy of 100% and it can be performed under solvent-free conditions hence displaying potentially low E-factors[16].

Although the reaction is thermodynamically favorable, since it uses epoxides as high energetic molecules to compensate for the high thermodynamic stability of carbon dioxide, a catalyst is needed to carry out the process under milder conditions. In this regard, several catalytic systems, both homogeneous and heterogeneous, have been developed including metal oxides[17-19], ionic liquids (ILs)[20-22], metal-organic frameworks (MOFs)[23-25], porous organic polymers (POPs)[26] and covalent organic frameworks (COFs)[2].

Homogeneous catalysts are usually highly active and selective however, they suffer from some disadvantages mainly related to their difficult reuse and to the laborious and time-consuming processes of isolation of cyclic carbonates from the reaction medium. These problems can be overcome by means of heterogeneous catalytic platforms that can allow easier recycling processes greatly increasing the sustainability of the reaction[27, 28]. CO_2 conversion into cyclic carbonates has been successfully obtained combining a Lewis acid and a nucleophile such as a halogen anion in the same bifunctional material[26, 29-32]. The simultaneous presence of both species provides a co-catalytic effect due to the Lewis Acid coordinating the oxygen of the three-membered ring and the nucleophile which favours the opening of the epoxide through the attack of the nucleophile[28].

Consequently, on the grounds of our experience with imidazolium salt-based catalysts for the conversion of CO_2 to cyclic carbonates[33-36], we designed a new bifunctional heterogeneous platform with an inorganic core based on polyhedral oligomeric silsesquioxanes (POSS). POSS are a class of organic-inorganic hybrid molecules made by an inorganic nanocaged silicate core surrounded by organic functional groups dangling in a three-dimensional arrangement. In addition, POSS based nanostructures display a good thermal and chemical stability and different applications[36-42]. The general formula of these hybrid molecules is $(R{-}SiO_{1.5})_n$, where n is commonly 6, 8, 10 and 12, the ratio O/Si is 1.5 and R is the vertex functional group (hydrogen, alkyl, alkene, aryl, arylene, etc.). The POSS with a T_8 cubic inorganic core composed of silicon-oxygen bonds ($R_8Si_8O_{12}$) is the most investigated nanostructure. These silica nanocages have been largely employed for the design of hybrid polymers and nanocomposites. POSS could be integrated into composites in different ways such as using an

octavinyl-POSS as functional monomer of the polymerization in order to produce a cross-linked polymeric network[43, 44]. Recently a very active bi-component material based on a copolymeric network of an imidazolium salt as nucleophilic source and a metal porphyrin complex as Lewis acid was synthetized and supported onto multi-walled carbon nanotubes[28].

With the aim of following the promising path of heterogeneous bifunctional materials and exploiting the proximity effect that POSS can exert [43, 44], two new catalytic materials were synthesized. The synthetic strategy involved the preparation of a 3D network by radical copolymerization of a tetrastyrylporphyrin aluminum chloride monomer (TSP_AlCl) with a bis-vinylimidazolium salt (bis-imiBr) carrying bromide anions as counter ion and the octavinylsisesquoxane as inorganic core building block.

All the materials prepared have been fully characterized by means of different analytic and spectroscopic techniques, and they have been tested in the synthesis of cyclic carbonates starting from CO_2 and several epoxides with excellent results.

2. Materials and methods

Octavinylsilsesquioxane, styrene oxide, epichlorohydrin and cyclohexene oxide were purchased from TCI. Glycidol and 2,2'-azobis(2-methylpropionitrile) (AIBN) and diethylaluminum chloride were purchased from Sigma-Aldrich. These chemicals were used without further purification. ^{1}H and ^{13}C NMR spectra were recorded on a Bruker 300 MHz spectrometer. Solid state ^{13}C and ^{29}Si NMR spectra were recorded at room temperature on a JEOL ECZ-R spectrometer operating at 14.1 T using a 3.2 mm automas probe and spinning frequencies of 10 kHz. X-ray photoelectron spectroscopy (XPS) analyses were carried out in a ThermoFisher ESCALAB 250Xi instrument. Thermogravimetric analysis was performed under nitrogen flow from 25 to 900 °C with a heating rate of 10 °C/min in a Mettler Toledo TGA STAR system. Transmission electron microscopy (TEM) images were obtained using a Philips Tecnai 10 microscope operating at 80 kV. The samples were prepared by dispersion of a small quantity

of the material in absolute ethanol and deposited into a copper grid. Inductively coupled plasma optical emission spectroscopy. (ICP-OES) was performed in an Optima 8000 ICP-OES spectrometer.

2.1. Synthetic procedures

*2.1.1. Synthesis of bis-vinylimidazolium salt (**bis-imiBr**)*

Bis-vinylimidazolium salt (**bis-imiBr)** was synthesized according to a reported procedure[28].

2.1.2. Synthesis of Tetrastyrylporphyrin

Tetrastyrylporphyrin (**TSP**) was synthesized according to a reported procedure [28]. After drying, the tetrastyrylporphyrin was obtained as a purple powder (415 mg; 27 %). ^{1}H NMR (300 MHz, $CDCl_3$, δ): 8.90 (s, 8 H), 8.19 (d, *J* = 7.9 Hz, 8 H), 7.81 (d, *J* = 8.0 Hz, 8 H), 7.07 (dd, *J* = 17.6, 10.9 Hz, 4 H), 6.08 (d, *J* = 17.6 Hz, 4 H), 5.51 (d, *J* = 10.9 Hz, 4 H), −2.73 (s, 2 H) ppm.

*2.1.3. Synthesis of tetrastyrylporphyrin aluminum chloride (**TSP_AlCl**)*

Tetrastyrylporphyrin aluminum chloride (**TSP_AlCl**) was synthesized according to a reported procedure[28]. **TSP_AlCl** was obtained as purple powder (115 mg; 53 %). ^{1}H NMR (300 MHz, $CDCl_3$, δ): 8.41 (s, 8 H), 7.49 (s, 16 H), 6.98 (dd, *J* = 17.6, 11.0 Hz, 4 H), 5.99 (d, *J*= 17.7 Hz, 4 H), 5.49 (d, *J* = 10.9 Hz, 4 H) ppm.

*2.1.4. Preparation of **POSS_TSP_AlCl***

In a 25 mL two-neck round-bottom flask, octavinylsilsesquioxane (100 mg, 0.158 mmol) and **TSP_AlCl** (200 mg, 0.25 mmol) were solubilized in dry DMF (6 mL) and sonicated for 10 min. Then, AIBN (49 mg, 0.294 mmol) was added under argon and the reaction mixture stirred for 30 min at room temperature before increasing up the temperature to 80 °C. After 24h the dark mixture obtained was

cooled at room temperature and transferred in a centrifuge tube by adding a small amount of DMF. The residue mixture was subjected to centrifugation several times with different solvents. Two times in DMF, three times using a methanol/Et_2O (v/v) 3/1 mixture and two times with Et_2O. The solid was recovered and dried under vacuum at 40 °C. **POSS_TSP_AlCl** was obtained as a dark powder (300mg).

*2.1.5. Preparation of **POSS_TSP_AlCl_imiBr***

In a 25 mL two-neck round-bottom flask, octavinylsilsesquioxane (150 mg, 0.237 mmol), **TSP_AlCl** (200 mg, 0.25 mmol), and **bis-imiBr** (404 mg, 1 mmol) were solubilized in dry DMF (8 mL) and sonicated for 10 min. Then, AIBN (108 mg, 0.657 mmol) was added under argon and the reaction mixture stirred for 30 min at room temperature before increasing up the temperature to 80 °C. After 24h the dark mixture obtained was transferred in a centrifuge tube by adding a small amount of DMF. The residue mixture was subjected to centrifugation several times with different solvents. Two times in DMF, three times using a methanol/Et_2O (v/v) 3/1 mixture and two times with Et_2O. The solid was recovered and dried under vacuum at 40 °C. **POSS_TSP_AlCl_imiBr** was obtained as a dark powder (660 mg).

2.2. Catalytic experiments

Catalytic experiments were carried out using a Cambridge Design Bullfrog batch reactor equipped with temperature control and mechanical stirring. In each test, the catalyst (see Table 1 for the corresponding amounts) and the proper epoxide (24 mL) were added to a Teflon vial and then the reactor was closed. After passing a flow of N_2 for 10 minutes and loading 25 bar of CO_2, the system was left to react at the target temperature reached by a ramp of 5 °C/min. In selected cases, a refill of CO_2 was carried out during the experiment. In these cases, the initial pressure of CO_2 was never overpassed. After the proper reaction time (3h or 24 h), the reactor was cooled down to room temperature, depressurized and, then, the catalyst was recovered from the reaction mixture by

centrifugation (15 min at 4500 or 9000 rpm). The supernatant was analyzed by ^{1}H NMR in d_6-DMSO. Each catalyst was dried overnight under vacuum at 60°C prior to the catalytic test.

2.3. Recycles

Recycling tests were carried out employing styrene oxide. At the end of the catalytic experiment, after separation the catalyst from the reaction mixture, a small amount of solvent (toluene, then ethanol and finally diethyl ether) was added to the solid and the mixture was sonicated for 15 minutes. Then, the material was recovered by centrifugation. The recovered solid was dried overnight in a vacuum oven at 60 °C. In order to maintain the same catalytic loading, the dried catalyst was weighed and reused in the same reaction, modifying, if necessary, the amount of epoxide.

2.4. Leaching test

Styrene oxide was used for leaching test. At the end of the catalytic cycle, the catalyst was recovered from the reaction mixture via centrifugation during 15 min at 4500 rpm and the supernatant was analyzed by ^{1}H NMR in d_6-DMSO. Then, the liquid mixture was filtered through a 0,2 μm filter and allowed to react again in the same reaction condition. During the reaction time, no decrease of the CO_2 pressure was observed and no further conversion was detected by ^{1}H NMR analysis.

3. Results and Discussion:

The tetrastyrylporphyrin alluminium chloride (**TSP_AlCl**) was obtained by reaction between tetrastyrylporphyrin and Et_2AlCl, as previously reported[28]. **TSP_AlCl** complex was subsequently copolymerised with octavinyl-POSS by using α-α'-azoisobutyronitrile (AIBN) as radical iniziator. The reactivity of vinyl groups in this radical reaction allowed obtaining the material **POSS_TSP_AlCl** and the material **POSS_TSP_AlCl_imiBr** when the polymerization process was carried out in presence of

the bis-vinylimidazolium salt (**bis-imiBr**). The synthesis of material **POSS_TSP_AlCl** containing only the Lewis acid species was performed to explore whether the simultaneous presence of both the nucleophilic species and the co-catalytic Lewis acid in the catalytic platform **POSS_TSP_AlCl_imiBr** may led to a synergic cooperation (**Scheme 1**).

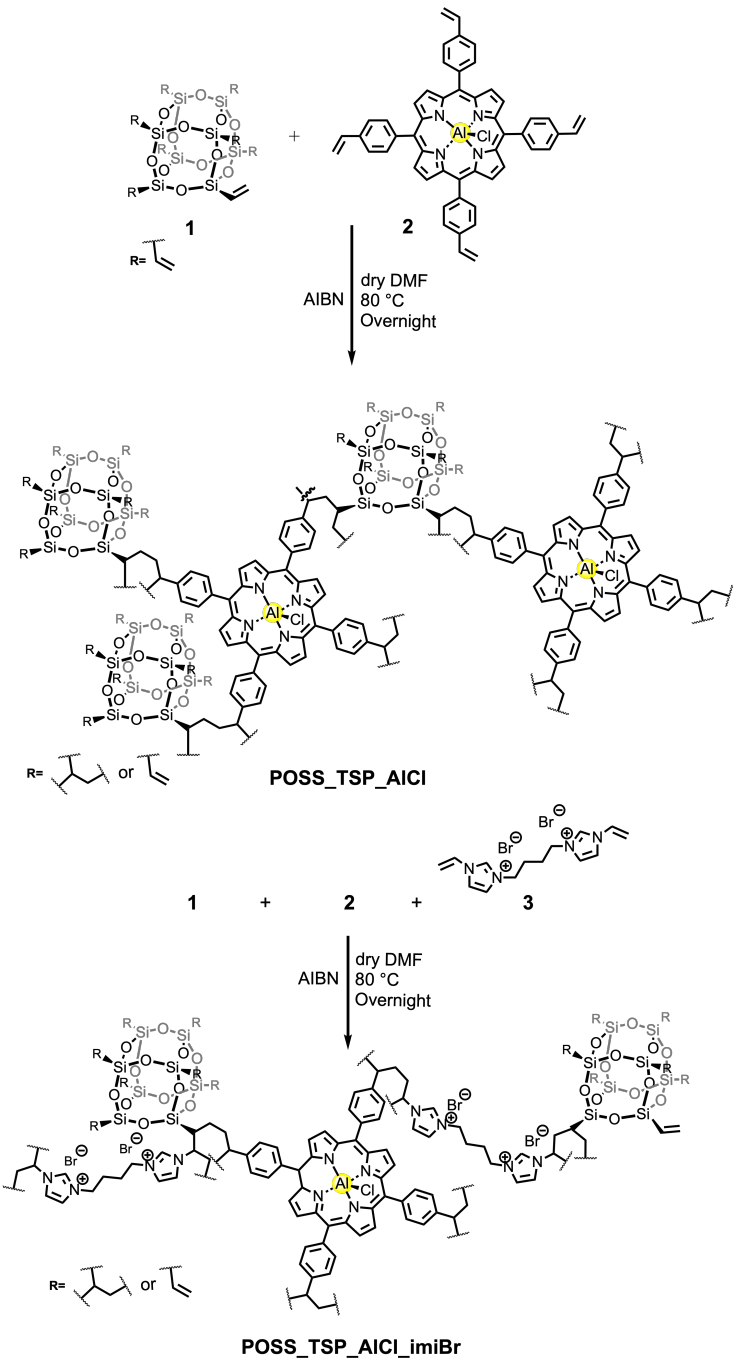

Scheme 1. Synthesis of **POSS_TSP_AlCl** and of **POSS_TSP_AlCl_imiBr**.

The two materials **POSS_TSP_AlCl** and **POSS_TSP_AlCl_imiBr** were characterized via different techniques including ^{13}C and ^{29}Si cross-polarization magic angle spinning (^{13}C and ^{29}Si CP-MAS) NMR spectroscopy. ^{29}Si solid state NMR spectra (**Figure 1**) of **POSS_TSP_AlCl_imiBr** and **POSS_TSP_AlCl** revealed the presence of two main contributions centred at -65 and -79 ppm which can be both assigned to the T8 POSS cage with condensed structure. The two signals can be attributed to the ^{29}Si atoms linked to alkyl groups of reacted vinyl moieties (alkyl-Si) and unreacted vinyl groups (vinyl-Si), respectively. This interpretation agrees with the NMR data of POSS structures previously reported in the literature[45].

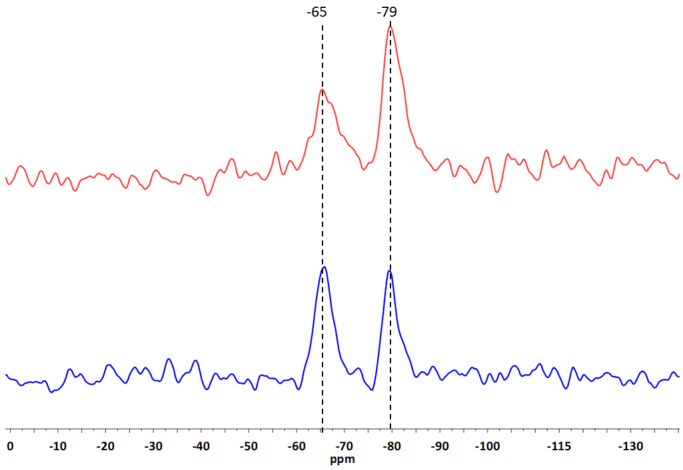

Figure 1. Solid state CP-MAS ^{29}Si NMR of **POSS_TSP_AlCl_imiBr** (Blue Line) and **POSS_TSP_AlCl** (Red Line).

^{13}C Solid state NMR spectra of both materials (**Figure 2**; **Figure S1**) display the signals attributed to the carbon atoms of the porphyrin together with those of the imidazolium moieties and not reacted vinyl groups in the 115-150 ppm region. The contributions present in the 20-60 ppm region are assigned to the aliphatic carbon atoms generated upon the polymerization process and those of the butyl linker between the two imidazolium moieties.

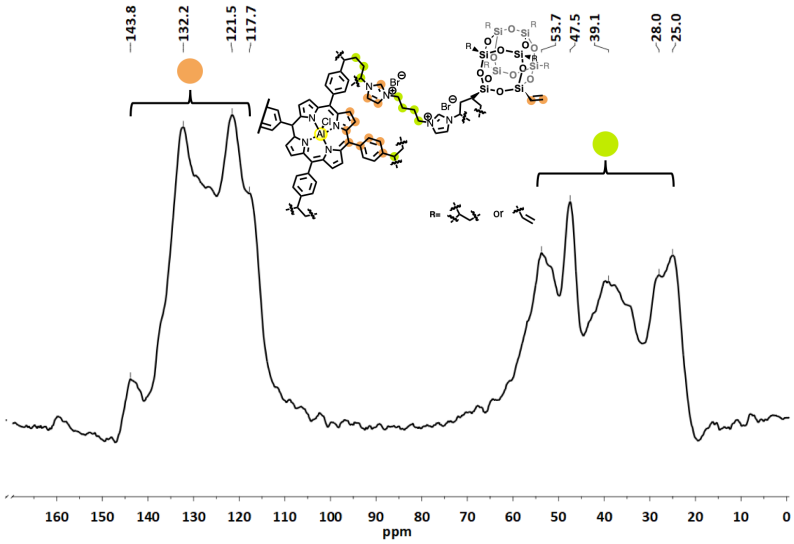

Figure 2. Solid state CP-MAS TOSS ^{13}C NMR of **POSS_TSP_AlCl_imiBr.**

Thermogravimetric analysis (TGA) was carried out on the two solids under N_2 flow (**Figure 3**). The solids display two different degradation profiles, showing appealing features for the reaction under study in this work. First, the presence of the imidazolium salt moieties in **POSS_TSP_AlCl_ImiBr** make it more hygroscopic than **POSS_TSP_AlCl**, justifying the weight loss between room temperature and 100 °C. Interestingly, the two materials present a good thermal stability up to 300 °C. After this temperature they start to decompose with a first weight loss at *c.a.* 320 °C and another one centered at *c.a.* 418 °C for **POSS_TSP_AlCl_imiBr**, and a degradation peak centered a 478 °C for **POSS_TSP_AlCl**, thus confirming the good thermal stability of both hybrids. The study of thermal behaviour of these two cross-linked nanohybrid materials is of central importance because of their possible recycling under the heating regimes.

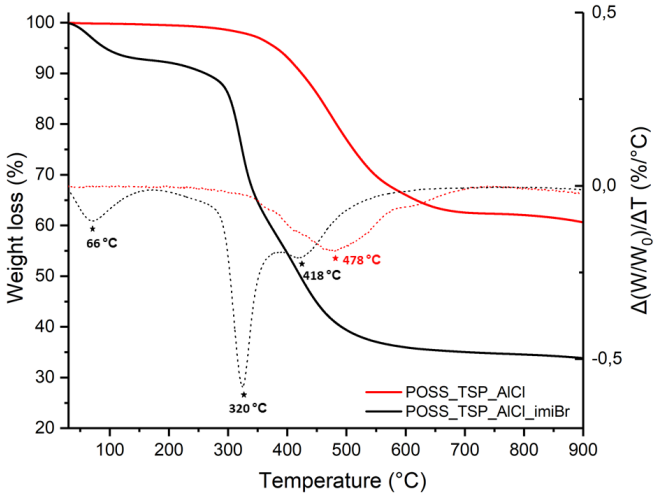

Figure 3. TGA (solid lines) and DTG (dotted lines) analysis in N_2 of **POSS_TSP_AlCl** and **POSS_TSP_AlCl_imiBr**.

X-ray photoelectron spectroscopy (XPS) was employed to understand the composition of the outer surface of the solids **POSS_TSP_AlCl** and **POSS_TSP_AlCl_imiBr** (**Figure 4** and **Figure S2**). In **Figure 4a** the XPS survey spectrum of **POSS_TSP_AlCl_imiBr** displays the presence of Al and Br derived from the TSP_AlCl and bis-imiBr monomers, respectively. **Figure 4b** shows the high-resolution XPS spectra of the N1s region of **POSS_TSP_AlCl_imiBr** which can be deconvoluted into two contributions at 399.4 and 401.7 eV with atomic percentages of 39 % and 61 %. These two signals can be attributed to the nitrogen atoms of the porphyrin ring coordinated with aluminum (Al–N) and the nitrogen atoms of the imidazolium rings, respectively[28]. On the other hand, the high-resolution XPS spectra of the N1s region of **POSS_TSP_AlCl** (**Figure S2b**) shows only one peak centred at 399.4 eV related to the nitrogen atoms of the porphyrin ring coordinated with aluminum (Al–N) which is the only type present in the material. The amount of aluminum present in **POSS_TSP_AlCl** and **POSS_TSP_AlCl_imiBr** was estimated by inductively-coupled plasma atomic emission spectroscopy (ICP-OES) analysis resulting 0.40 and 0.32 mmol/g, respectively.

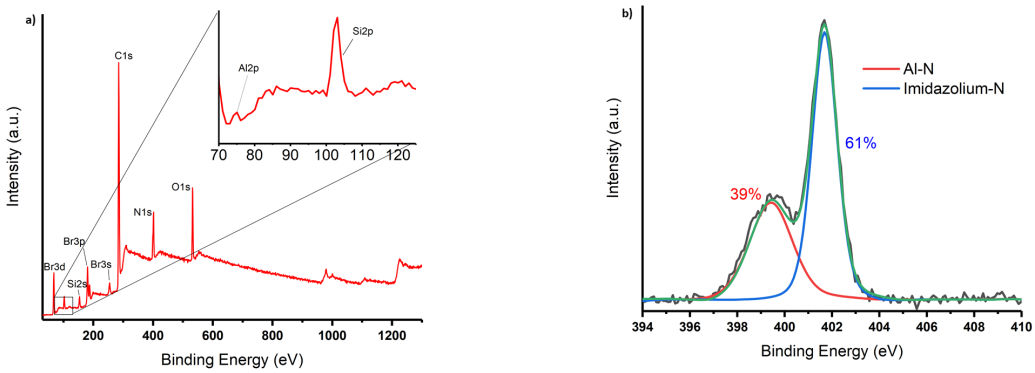

Figure 4. XPS Survey (a) and N1s High resolution (b) of **POSS_TSP_AlCl_imiBr**

Finally, the morphology of the two catalysts **POSS_TSP_AlCl** and **POSS_TSP_AlCl_imiBr** was studied by using trasmission electron microscopy (TEM) (**Figure 5**). TEM images showed that the two materials display irregular and amorphous porous structures with an accessible polymeric network.

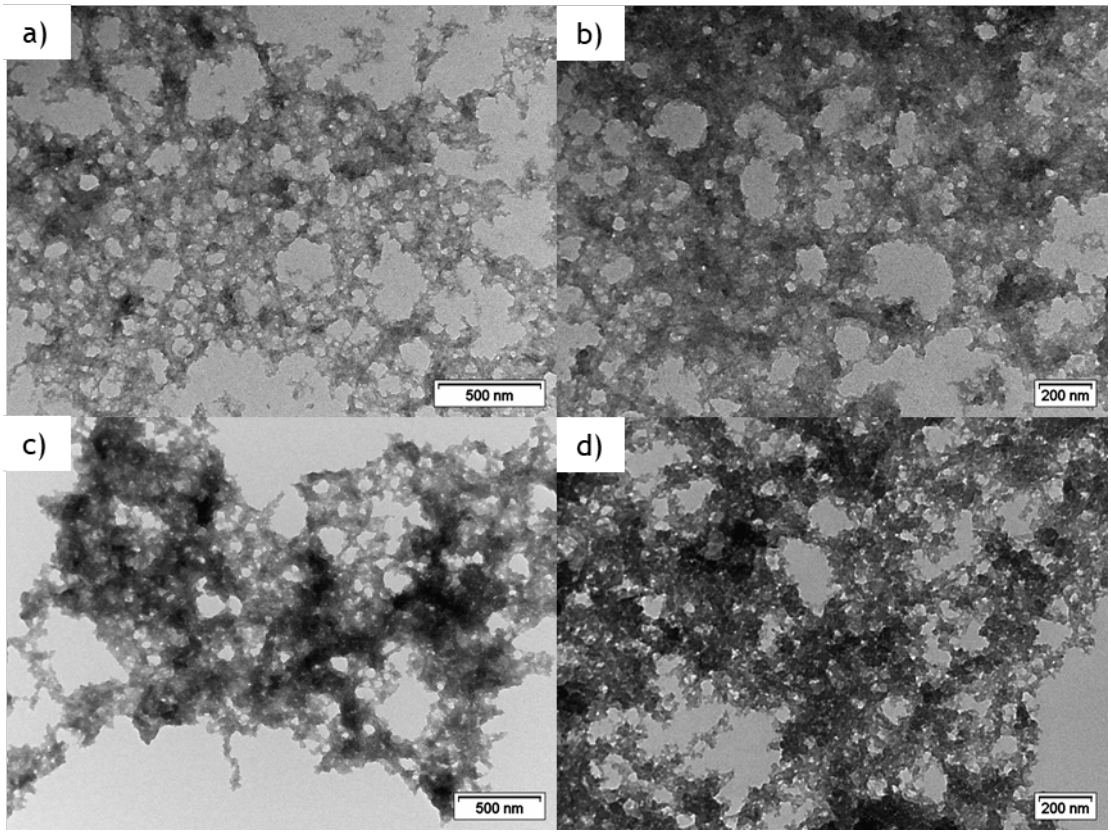

Figure 5. TEM images of **POSS_TSP_AlCl_imiBr** (a,b) and **POSS_TSP_AlCl** (c,d).

Once characterised, both materials were investigated in the conversion of carbon dioxide to cyclic carbonates by employing styrene oxide as benchmark reactant under solvent-free conditions. Due to the different content of active species in the two materials, a more specific comparison of the catalytic activity of **POSS_TSP_AlCl** and **POSS_TSP_AlCl_imiBr** solids was performed considering the turnover number values based on the aluminum content (TON_{Al}; defined as moles of epoxide converted/moles of Al active sites) (**Scheme 2**).

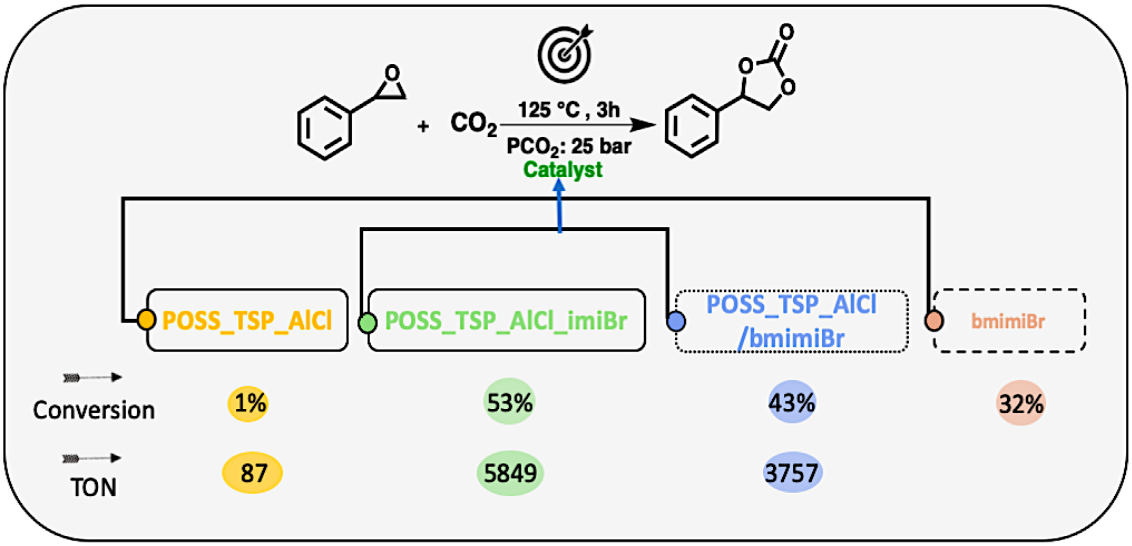

Scheme 2. Comparison of the catalytic activity of **POSS_TSP_AlCl** (60 mg ; 0,024 mmol Al) and **POSS_TSP_AlCl_imiBr** (60 mg 0,019 mmol Al), **POSS_TSP_AlCl/bmimBr** (0,024 mmol Al, 1:6 molar ratio) and **bmimBr** (30 mg) in the reaction of styrene oxide with CO_2. Reaction conditions: styrene oxide (209.7 mmol), catalyst (0.024 or 0.019mmol Al) , 25 bar CO_2, 125 °C, 3 h, 500 rpm.

Initially, **POSS_TSP_AlCl** and **POSS_TSP_AlCl_imiBr** were tested in the reaction using the same mass amount obtaining a very different conversion of 1% and 53%, respectively (**Scheme 2**). The huge difference between the two reactions is ascribed to the absence of a nucleophilic source in **POSS_TSP_AlCl**, resulting thus essential in the target process. Two additional tests were performed:

the first employing **POSS_TSP_AlCl** (0.024 mmol Al), as source of Lewis acid species, combined with butylmethylimidazolium bromide salt (**bmimBr,** molar ratio 1:6), as the nucleophile source, and the second with **bmimBr** alone. It is worth to note that the former test displayed a higher conversion (43%) than the **bmimBr** alone (32%) but a TON sensibly lower (3757) than that obtained with the bifunctional heterogeneous system. The enhanced catalytic performances of the **POSS_TSP_AlCl_imiBr** catalyst could be ascribed to the proximity between the porphyrin core and the bis-vinylimidazolium in the 3D polymeric network. This proximity allows a cooperation between the two co-catalytic species which act synergistically during the catalytic cycle. A similar synergistic activation was previously reported in the literature[28].

Afterwards, the promising bifunctional material was employed with styrene oxide to study the recyclability of the catalyst. Five consecutive runs were performed and after each cycle the material was easily recovered from the reaction mixture by centrifugation, washed with toluene, ethanol and diethyl ether and dried under vacuum at 60°C overnight. The results shown in **Figure 6** indicate that **POSS_TSP_AlCl_imiBr** is a quite robust material under the selected reaction conditions and can be used for multiple cycles without any decrease of catalytic activity. Moreover, in order to confirm the absence of leached active species in the solution after the catalytic test, a further experiment was carried out. After the separation of **POSS_TSP_AlCl_imiBr** from the reaction mixture, the liquid phase was filtered using a 0.2 µm filter and was allowed to react under the same reaction conditions., An almost constant CO_2 pressure was detected during the reaction time (**Figure S3**), and the ^{1}H-NMR analysis at the end of the reaction showed only a small increase in conversion of 1.4%, confirming the absence of leached species.

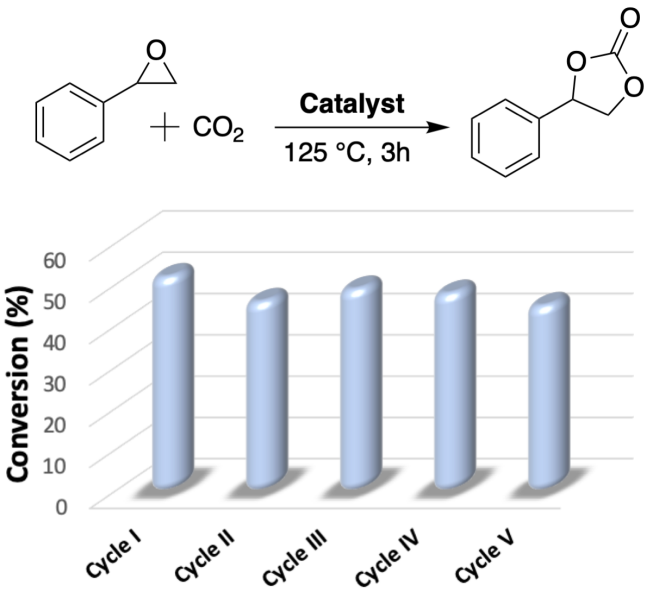

Figure 6. Recycling tests of **POSS_TSP_AlCl_imiBr**. Reaction conditions: styrene oxide (209.7 mmol), 60 mg of catalyst (0.019 mmol Al, 0.009 mol%), 25 bar of CO_2, 3h, 500 rpm.

The catalytic activity of **POSS_TSP_AlCl_imiBr** was also assessed using different epoxides (**Table 1**). Styrene oxide was converted into the corresponding cyclic carbonate with 53% of conversion when the material was employed at 125 °C for 3 h (Table 1, entry 1 and Scheme 2). Conversions of 44 % or 41% were obtained for glycidol at 50 °C in 3 h when an initial pressure of 25 bar or a constant pressure of 10 bar was applied, respectively (entries 2 and 3). Moreover, decreasing the temperature from 50 °C to 30 °C allows converting the 16% of glycidol in only 3 h (entry 4).

Epichlorohydrin was tested at different temperature: 100, 80 and 50 °C applying a reaction time of 3 h. A Conversion value of 91% was obtained at 100 °C in 3h (entry 5). Interestingly, a full conversion (>95%) of epichlorohydrin was obtained in the same conditions when the system was refilled with CO_2 after 1h (entry 6). Refilling the reagent in the gas phase after 1 h re-establishes good reaction kinetics as shown in **Figure S11,** where the comparison between the pressure profile during the reaction time of entries 5 and 6 shows how the kinetic of the process decreases during the consumption of CO_2.

Decreasing the temperature to 80 °C and 50 °C results in conversion values of 73% and 11%, respectively (entries 7 and 8).

A final step forward on the catalytic activity of **POSS_TSP_AlCl_imiBr** was made by recycling the material and subjecting it to different reaction conditions during catalysis between CO_2 and several more challenging-to-convert epoxides.

As shown in **Table 1** good conversions were obtained for cyclohexene oxide and oxetane at the first and the second reuse of the material. In the former case, a conversion of 88% was reached in 24h at 150 °C employing 100 mg (0.032 mmol of Al) of catalyst (entry 9). Despite the good conversion, *cis*-cyclohexane carbonate was not the only product obtained. During the reaction also *trans*-cyclohexane carbonate and the poly-cyclohexane carbonate were formed with a selectivity toward cyclic carbonates of 83 % and *cis*/*trans* ratio of 72:28 (**Figure S10**).[46] On the other hand, >95% of oxetane was converted in 24h at 150 °C with a full selectivity toward the corresponding polycarbonate (entry 10). This result agrees with the selectivity reported in the literature in the conversion of CO_2 by addition to oxetane when the coordinating metal is aluminum[47]. To better evaluate the robustness of the material after recycling, epichlorohydrin was tested again in the same condition of Entry 5. A slightly decreased conversion (73%) was observed when the reused material was employed with respect to the reaction carried out in the presence of the fresh catalyst (entry 5).

Even with this diminished conversion, the material remains still active and quite efficient even after several consecutive uses under different reaction conditions contributing thus to making this class of materials promising for the conversion of CO_2 in cyclic carbonate.

Table 1. Reaction conditions of different screening tests of **POSS_TSP_AlCl_imiBr** with different epoxides.

Entry	Tests	Substrate	Temperature (°C)	Conversion[a] (%)	TON_{Al} [b]	TOF_{Al} [b]	Productivity [c] (P)
1	I cycle	Styrene oxide (209.7 mmol)	125	53	5849	1950	211
2	I cycle	Glycidol (379 mmol)	50	44	8777	2926	328
3[d]	I cycle	Glycidol (379 mmol)	50	41	8178	2726	306
4	I cycle	Glycidol (379 mmol)	30	16	3192	1064	119
5	I cycle	Epichlorohydrin (306 mmol)	100	91	14656	4885	634
6[e]	I cycle	Epichlorohydrin (306 mmol)	100	>95	16105	5368	696
7	I cycle	Epichlorohydrin (306 mmol)	80	73	11756	3919	508
8	I cycle	Epichlorohydrin (306 mmol)	50	11	1772	591	77
9[f]	II cycle	Cyclohexene oxide (237 mmol)	150	88[g]	6518	272	296
10[h]	III cycle	Oxetane (372 mmol)	150	>95[h]	18600	775	386
11	IV cycle	Epichlorohydrin (306 mmol)	100	73	11596	3865	501

Reaction conditions: 24 mL of epoxides, 60 mg of catalyst (0,019 mmol Al), 25 Bar of CO_2, 3h, 500 rpm.

[a] Determined by ^1H NMR (figure S4; S7 to S10)

[b] TON and TOF values calculated on the basis of the Al content estimated by ICP analysis. (TON = mmol epoxide converted/ mmol Al); (TOF= TON/ time (h))

[c] Productivity (P)= grams of product/grams catalyst considering 100 % selectivity

[d] Constant pressure of 10 bar of CO_2

[e] Refill at 40 bar of CO_2 after 1h of reaction time.

[f] 100 mg of catalyst (0.032 mmol Al); reaction time of 24h

[g] Selectivity toward cyclic carbonates 83 % (cis/trans ratio 72:28).

[h] Reaction time of 24h; selectivity 99% toward polycarbonate.

Finally, a comparison with other catalytic systems is usually carried out; however, the reaction under examination has different experimental parameters and a close comparison is difficult to do. Aluminum-based catalysts are largely investigated for the above reaction but we believe that a comparison should be made with bifunctional supported catalytic systems. In Table 2 are reported

few examples. First we examined **POSS_TSP_AlCl_imiBr** and **MWCNT-TSP-AlCl-imi**, a previous material prepared by our group that was used under the same reaction conditions. Both materials possess the Al-porphyrin-imidazolium cross-linked network but on different support, POSS and MWCNT respectively. The MWCNT-based material performs slightly better with styrene oxide compared to the POSS-based catalyst (entries 1-2); the MWCNT performs better with epichlorohydrin in terms of conversion and TON values, though they showed similar productivity values (entries 7-8); on the other hand, the POSS-based catalyst showed a very interesting result with the less reactive cyclohexene oxide in terms of conversion and selectivity toward the cyclic carbonate, TON and productivity values (entries 13-14). The latter two values, calculated on selectivity towards cyclic carbonate highlight the greater performance of the POSS-based catalyst. Catalytic materials based on bifunctional Al-porphyrin/imidazolium bromide system (Al-iPOP-1) or Al-salen/imidazolium bromide system (COP-Al) gave high conversions at milder conditions but using a large amount of catalytic materials as demonstrated by the productivity values (entries 3,4,9,10,15). The synergy between the metal center (Lewis acid) and the co-catalyst (halide ion) in **POSS_TSP_AlCl_imiBr** allows achieving enhanced catalytic performances with respect to POSS-based catalysts that do not contain Lewis acid. In the case of IM-iPHP-2 and V-iPHP-1 the reaction was assisted by many H-bondings. In these cases, the materials did not present a silica nanocage with a fully condensed (T8) arrangement, but it was shown that part of the cage was hydrolysed. This opening of the cubic structure led to the formation of silanol groups that can make a contribution to catalysis through hydrogen bonding between the hydrogen of the hydroxyl groups attached to the silicon atom and the oxygen of the epoxide.

Table 2. Selected data for the reaction between epoxides and CO_2 in the presence of different catalytic systems.

Entry	Catalyst	Substrate	Conv. (%)	TON_{Al}	P[a]	Reaction condition	Ref.
1	POSS_TSP_AlCl_imiBr	Styrene oxide	53	5849	211	25 bar; 3h; 125 °C	This Work
2	MWCNT-TSP-AlCl-imi	Styrene oxide	55	7649	316	25 bar; 3h; 125 °C	[28]
3	Al-iPOP-1	Styrene oxide	52		51	1 MPa; 9 h; 40 °C	[48]
4	COP-Al	Styrene oxide	91.5		50	1 MPa; 18 h; 90 °C	[49]
5	IM-iPHP-2	Styrene oxide	84		5.5	1 bar; 72 h; 80 °C	[50]
6	V-iPHP-1	Styrene oxide	93		6.1	0.1 MPa; 72 h; 80 °C	[51]
7	POSS_TSP_AlCl_imiBr	Epichlorohydrin	91	14656	634	25 bar; 3h; 100 °C	This Work
8	MWCNT-TSP-AlCl-imi	Epichlorohydrin	>95	20265	661	25 bar; 3h; 100 °C	[28]
9	Al-iPOP-1	Epichlorohydrin	99		81	10 bar; 6h; 40°C	[48]
10	COP-Al	Epichlorohydrin	98		45	10 bar; 18h; 90°C	[49]
11	IM-iPHP-2	Epichlorohydrin	96		5.2	0.1 MPa; 48 h; 80 °C	[50]
12	V-iPHP-1	Epichlorohydrin	97		5.3	0.1 MPa; 48 h; 80 °C	[51]
13	POSS_TSP_AlCl_imiBr	Cyclohexene oxide	88[b]	6518[d]	296[e]	25 bar; 24 h; 150 °C	This work
14	MWCNT-TSP-AlCl-imi	Cyclohexene oxide	71[c]	3352[d]	119[e]	25 bar; 24 h; 150 °C	[28]
15	Al-iPOP-1	Cyclohexene oxide	83		71	10 bar; 36 h; 40°C	[48]

[a] Productivity(P)= grams of product/grams catalyst; [b] selectivity toward cyclic carbonate, 83%; [c] selectivity toward cyclic carbonate, 74%; [e] TON based on cyclic carbonate: 5410 and 2480 respectively. [d] Productivity based on cyclic carbonate: 245 and 88 respectively.

4. Conclusions

Octavinylsilsesquioxane and aluminum chloride tetrastyrylporphyrin (**TSP_AlCl**) have been subjected to AIBN mediated radical polymerization in the presence (**POSS_TSP_AlCl_imiBr**) and in absence (**POSS_TSP_AlCl**) of and bis-vinylimidazolium dibromide (**bis-imiBr**). The corresponding cross-linked solids have been thoroughly characterized by means of several spectroscopic and analytic techniques such as TGA, ICP-OES, XPS, TEM, solid state NMR. Hybrid materials were used as heterogeneous catalysts in the cycloaddition reaction of CO_2 with epoxides to obtain the corresponding cyclic carbonates under solvent-free conditions. It has been shown how the presence of both Lewis acid and nucleophilic species within the same heterogeneous material **POSS_TSP_AlCl_imiBr** leads to a catalyst with high catalytic performance due to the synergistic effects exerted by the metal centers and halide ions. This performance could be ascribed to a

twofold effect. A first contribution is attributed to the close proximity between the metal centers and the bromide ions, which are able to cooperate and exert a synergistic effect during the catalytic cycle. A second contribution comes from the use of the POSS-silica nanocage used as a building block during synthesis. The possibility of functionalizing the POSS cage at its vertices ensures an increase in the concentration of active sites in the material at certain localized positions. The hybrid catalyst showed high catalytic activity with a range of different epoxides, with TON and TOF values of up to 16,000 and 5,000, respectively. **POSS_TSP_AlCl_imiBr** was easily recoverable and recyclable for at least five cycles with unchanged activity, and no leaching phenomena have been observed during the performed tests. Based on these results, different catalytic systems can be easily designed by changing both the nature of metalloporphyrin and/or halide ion as well as the linker of the bis-imidazolium salt.

Acknowledgements

This research was funded by University of Palermo and the Italian Ministry of Education (PRIN 2017 project no. 2017W8KNZW). This research is supported by the F.R.S-FNRS via funding grants GEQ U.G014.19 EQP U.N034.17 and PDR T.0004.21. A. M. gratefully acknowledges the University of Palermo and University of Namur for a co-funded PhD fellowship.

References

[1] Full J, Ziehn S, Geller M, Miehe R, Sauer A. Carbon-negative hydrogen production: Fundamentals for a techno-economic and environmental assessment of HyBECCS approaches. GCB Bioenergy 2022;14(5):597-619. https://doi.org/10.1111/gcbb.12932.

[2] Ozdemir J, Mosleh I, Abolhassani M, Greenlee LF, Beitle RR, Beyzavi MH. Covalent Organic Frameworks for the Capture, Fixation, or Reduction of CO2. Front Energy Res 2019;7:77. https://doi.org/10.3389/fenrg.2019.00077.

[3] Sakakura T, Choi J-C, Yasuda H. Transformation of Carbon Dioxide. Chem Rev 2007;107(6):2365-87. https://doi.org/10.1021/cr068357u.

[4] Rahman FA, Aziz MMA, Saidur R, Bakar WAWA, Hainin MR, Putrajaya R, et al. Pollution to solution: Capture and sequestration of carbon dioxide (CO2) and its utilization as a renewable energy source for a sustainable future. Renewable Sustainable Energy Rev 2017;71:112-26. https://doi.org/10.1016/j.rser.2017.01.011.

[5] Liu Q, Wu L, Jackstell R, Beller M. Using carbon dioxide as a building block in organic synthesis. Nat Commun 2015;6(1):5933. https://doi.org/10.1038/ncomms6933.
[6] Aresta M, Dibenedetto A, Angelini A. Catalysis for the Valorization of Exhaust Carbon: from CO2 to Chemicals, Materials, and Fuels. Technological Use of CO2. Chem Rev 2014;114(3):1709-42. https://doi.org/10.1021/cr4002758.
[7] Luo R, Liu X, Chen M, Liu B, Fang Y. Recent Advances on Imidazolium-Functionalized Organic Cationic Polymers for CO2 Adsorption and Simultaneous Conversion into Cyclic Carbonates. ChemSusChem 2020;13(16):3945-66. https://doi.org/10.1002/cssc.202001079.
[8] Calabrese C, Liotta LF, Giacalone F, Gruttadauria M, Aprile C. Supported Polyhedral Oligomeric Silsesquioxane-Based (POSS) Materials as Highly Active Organocatalysts for the Conversion of CO2. ChemCatChem 2019;11(1):560-7. https://doi.org/10.1002/cctc.201801351.
[9] Saptal VB, Bhanage BM. Current advances in heterogeneous catalysts for the synthesis of cyclic carbonates from carbon dioxide. Curr Opin Green Sustainable Chem 2017;3:1-10. https://doi.org/10.1016/j.cogsc.2016.10.006.
[10] Clegg W, Harrington RW, North M, Pizzato F, Villuendas P. Cyclic carbonates as sustainable solvents for proline-catalysed aldol reactions. Tetrahedron: Asymmetry 2010;21(9):1262-71. https://doi.org/10.1016/j.tetasy.2010.03.051.
[11] Pescarmona PP. Cyclic carbonates synthesised from CO2: Applications, challenges and recent research trends. Curr Opin Green Sustainable Chem 2021;29:100457. https://doi.org/10.1016/j.cogsc.2021.100457.
[12] Kamphuis AJ, Picchioni F, Pescarmona PP. CO2-fixation into cyclic and polymeric carbonates: principles and applications. Green Chem 2019;21(3):406-48. https://doi.org/10.1039/C8GC03086C.
[13] Pescarmona PP, Taherimehr M. Challenges in the catalytic synthesis of cyclic and polymeric carbonates from epoxides and CO2. Catal Sci Technol 2012;2(11):2169-87. https://doi.org/10.1039/C2CY20365K.
[14] Sheldon RA, Arends I, Hanefeld U. Green chemistry and catalysis. Weinheim, Germany: Wiley-VCH; 2015.
[15] Lancaster M. Green chemistry An introductory text. Cambridge, UK: Royal Society of Chemistry; 2002.
[16] Calabrese C, Giacalone F, Aprile C. Hybrid Catalysts for CO2 Conversion into Cyclic Carbonates. Catalysts 2019;9(4):325. https://doi.org/10.3390/catal9040325.
[17] Bhanage BM, Fujita S-i, Ikushima Y, Arai M. Synthesis of dimethyl carbonate and glycols from carbon dioxide, epoxides, and methanol using heterogeneous basic metal oxide catalysts with high activity and selectivity. Appl Catal, A 2001;219(1):259-66. https://doi.org/10.1016/S0926-860X(01)00698-6.
[18] Kulal N, Vasista V, Shanbhag GV. Identification and tuning of active sites in selected mixed metal oxide catalysts for cyclic carbonate synthesis from epoxides and CO2. J CO2 Util 2019;33:434-44. https://doi.org/10.1016/j.jcou.2019.07.018.
[19] Prasad D, Patil KN, Dateer RB, Kim H, Nagaraja BM, Jadhav AH. Basicity controlled MgCo2O4 nanostructures as catalyst for viable fixation of CO2 into epoxides at atmospheric pressure. Chem Eng J 2021;405:126907. https://doi.org/10.1016/j.cej.2020.126907.
[20] Girard A-L, Simon N, Zanatta M, Marmitt S, Gonçalves P, Dupont J. Insights on recyclable catalytic system composed of task-specific ionic liquids for the chemical fixation of carbon dioxide. Green Chem 2014;16(5):2815-25. https://doi.org/10.1039/C4GC00127C.
[21] Wang J, Leong J, Zhang Y. Efficient fixation of CO2 into cyclic carbonates catalysed by silicon-based main chain poly-imidazolium salts. Green Chem 2014;16(10):4515-9. https://doi.org/10.1039/C4GC01060D.

[22] Saptal VB, Bhanage BM. Bifunctional ionic liquids for the multitask fixation of carbon dioxide into valuable chemicals. ChemCatChem 2016;8(1):244-50. https://doi.org/10.1002/cctc.201501044.
[23] Liang J, Huang Y-B, Cao R. Metal–organic frameworks and porous organic polymers for sustainable fixation of carbon dioxide into cyclic carbonates. Coord Chem Rev 2019;378:32-65. https://doi.org/10.1016/j.ccr.2017.11.013.
[24] Nguyen PT, Nguyen HT, Nguyen HN, Trickett CA, Ton QT, Gutiérrez-Puebla E, et al. New metal–organic frameworks for chemical fixation of CO2. ACS Appl Mater Interfaces 2018;10(1):733-44. https://doi.org/10.1021/acsami.7b16163.
[25] Gao WY, Chen Y, Niu Y, Williams K, Cash L, Perez PJ, et al. Crystal engineering of an nbo topology metal–organic framework for chemical fixation of CO2 under ambient conditions. Angew Chem Int Ed 2014;53(10):2615-9. https://doi.org/10.1002/anie.201309778.
[26] Wang W, Li C, Yan L, Wang Y, Jiang M, Ding Y. Ionic liquid/Zn-PPh3 integrated porous organic polymers featuring multifunctional sites: highly active heterogeneous catalyst for cooperative conversion of CO2 to cyclic carbonates. ACS Catal 2016;6(9):6091-100. https://doi.org/10.1021/acscatal.6b01142.
[27] Singh Dhankhar S, Ugale B, Nagaraja C. Co-Catalyst-Free Chemical Fixation of CO2 into Cyclic Carbonates by using Metal-Organic Frameworks as Efficient Heterogeneous Catalysts. Chem Asian J 2020;15(16):2403-27. https://doi.org/10.1002/asia.202000424.
[28] Campisciano V, Valentino L, Morena A, Santiago-Portillo A, Saladino N, Gruttadauria M, et al. Carbon nanotube supported aluminum porphyrin-imidazolium bromide crosslinked copolymer: A synergistic bifunctional catalyst for CO2 conversion. J CO2 Util 2022;57:101884. https://doi.org/10.1016/j.jcou.2022.101884.
[29] Liu T-T, Liang J, Huang Y-B, Cao R. A bifunctional cationic porous organic polymer based on a Salen-(Al) metalloligand for the cycloaddition of carbon dioxide to produce cyclic carbonates. Chem Commun 2016;52(90):13288-91. https://doi.org/10.1039/C6CC07662A.
[30] Ema T, Miyazaki Y, Taniguchi T, Takada J. Robust porphyrin catalysts immobilized on biogenous iron oxide for the repetitive conversions of epoxides and CO 2 into cyclic carbonates. Green Chem 2013;15(9):2485-92. https://doi.org/10.1039/C3GC41055B.
[31] Naveen K, Ji H, Kim TS, Kim D, Cho D-H. C3-symmetric zinc complexes as sustainable catalysts for transforming carbon dioxide into mono-and multi-cyclic carbonates. Appl Catal, B 2021;280:119395. https://doi.org/10.1016/j.apcatb.2020.119395.
[32] Seo YH, Hyun YB, Lee HJ, Lee HC, Lee JH, Jeong SM, et al. CO2/Propylene Oxide Copolymerization with a Bifunctional Catalytic System Composed of Multiple Ammonium Salts and a Salen Cobalt Complex Containing Sulfonate Anions. Macromol Res 2021;29(12):855-63. https://doi.org/10.1007/s13233-021-9094-4.
[33] Morena A, Campisciano V, Comès A, Liotta LF, Gruttadauria M, Aprile C, et al. A Study on the Stability of Carbon Nanoforms–Polyimidazolium Network Hybrids in the Conversion of CO2 into Cyclic Carbonates: Increase in Catalytic Activity after Reuse. Nanomaterials 2021;11(9):2243. https://doi.org/10.3390/nano11092243.
[34] Bivona LA, Fichera O, Fusaro L, Giacalone F, Buaki-Sogo M, Gruttadauria M, et al. A polyhedral oligomeric silsesquioxane-based catalyst for the efficient synthesis of cyclic carbonates. Catal Sci Technol 2015;5(11):5000-7. https://doi.org/10.1039/C5CY00830A.
[35] Buaki-Sogó M, Vivian A, Bivona LA, García H, Gruttadauria M, Aprile C. Imidazolium functionalized carbon nanotubes for the synthesis of cyclic carbonates: reducing the gap between homogeneous and heterogeneous catalysis. Catal Sci Technol 2016;6(24):8418-27. https://doi.org/10.1039/C6CY01068G.
[36] Calabrese C, Liotta LF, Carbonell E, Giacalone F, Gruttadauria M, Aprile C. Imidazolium-Functionalized Carbon Nanohorns for the Conversion of Carbon Dioxide: Unprecedented Increase of Catalytic Activity after Recycling. ChemSusChem 2017;10(6):1202-9. https://doi.org/10.1002/cssc.201601427.

[37] Ghanbari H, Cousins BG, Seifalian AM. A nanocage for nanomedicine: polyhedral oligomeric silsesquioxane (POSS). Macromol Rapid Commun 2011;32(14):1032-46. https://doi.org/10.1002/marc.201100126.
[38] Duszczak J, Mituła K, Santiago-Portillo A, Soumoy L, Rzonsowska M, Januszewski R, et al. Double-Decker Silsesquioxanes Self-Assembled in One-Dimensional Coordination Polymeric Nanofibers with Emission Properties. ACS Appl Mater Interfaces 2021;13(19):22806-18. https://doi.org/10.1021/acsami.1c02510.
[39] Jagannathan JR, Targos K, Franz AK. Synthesis of Functionalized Silsesquioxane Nanomaterials by Rhodium-Catalyzed Carbene Insertion into Si−H Bonds. Angew Chem Int Ed 2022;61(1). https://doi.org/10.1002/anie.202110417.
[40] Abudukelimu S, Wei G, Huang J, Zhao G, Wei L, Cui W, et al. Polyhedral oligomeric silsesquioxane (POSS)-based hybrid nanocomposite for synergistic chemo-photothermal therapy against pancreatic cancer. Chem Eng J 2022;442:136124. https://doi.org/10.1016/j.cej.2022.136124.
[41] Muhammad S, Niazi JH, Shawuti S, Qureshi A. Functional POSS based polyimide nanocomposite for enhanced structural, thermal, antifouling and antibacterial properties. Mater Today Commun 2022;31. https://doi.org/10.1016/j.mtcomm.2022.103287.
[42] Nowacka M, Kowalewska A. Self-Healing Silsesquioxane-Based Materials. Polymers 2022;14(9). https://doi.org/10.3390/polym14091869.
[43] Calabrese C, Aprile C, Gruttadauria M, Giacalone F. POSS nanostructures in catalysis. Catal Sci Technol 2020;10(22):7415-47. https://doi.org/10.1039/D0CY01407A.
[44] Calabrese C, Fusaro L, Liotta LF, Giacalone F, Comès A, Campisciano V, et al. Efficient Conversion of Carbon Dioxide by Imidazolium-Based Cross-Linked Nanostructures Containing Polyhedral Oligomeric Silsesquioxane (POSS) Building Blocks. ChemPlusChem 2019;84(10):1536-43. https://doi.org/10.1002/cplu.201900408.
[45] Zhao H, Shu J, Chen Q, Zhang S. Quantitative structural characterization of POSS and octavinyl-POSS nanocomposites by solid state NMR. Solid State Nucl Magn Reson 2012;43-44:56-61. https://doi.org/10.1016/j.ssnmr.2012.02.005.
[46] Cozzolino M, Melchionno F, Santulli F, Mazzeo M, Lamberti M. Aldimine-Thioether-Phenolate Based Mono-and Bimetallic Zinc Complexes as Catalysts for the Reaction of CO2 with Cyclohexene Oxide. Eur J Inorg Chem 2020;2020(17):1645-53. https://doi.org/10.1002/ejic.202000119.
[47] Honda M, Nakamura R, Sugimoto H. Copolymerization of carbon dioxide and oxetane catalyzed by aluminum porphyrin complex system. J Polym Sci 2021;59(24):3122-30. https://doi.org/10.1002/pol.20210536.
[48] Chen Y, Luo R, Xu Q, Jiang J, Zhou X, Ji H. Charged Metalloporphyrin Polymers for Cooperative Synthesis of Cyclic Carbonates from CO2 under Ambient Conditions. ChemSusChem 2017;10(11):2534-41. https://doi.org/10.1002/cssc.201700536.
[49] Zhang R-Y, Zhang Y, Tong J, Liu L, Han Z-B. A Bifunctional Cationic Covalent Organic Polymer for Cooperative Conversion of CO2 to Cyclic Carbonate without Co-catalyst. Catal Lett 2021;151(10):2833-41. https://doi.org/10.1007/s10562-021-03534-7.
[50] Chen G, Zhang Y, Xu J, Liu X, Liu K, Tong M, et al. Imidazolium-based ionic porous hybrid polymers with POSS-derived silanols for efficient heterogeneous catalytic CO2 conversion under mild conditions. Chem Eng J 2020;381:122765. https://doi.org/10.1016/j.cej.2019.122765.
[51] Zhang Y, Liu K, Wu L, Zhong H, Luo N, Zhu Y, et al. Silanol-Enriched Viologen-Based Ionic Porous Hybrid Polymers for Efficient Catalytic CO2 Fixation into Cyclic Carbonates under Mild Conditions. ACS Sustain Chem Eng 2019;7(19):16907-16. https://doi.org/10.1021/acssuschemeng.9b04627.

Supporting Information

POSS-Al-porphyrin-imidazolium cross-linked network as catalytic bifunctional platform for the conversion of CO_2 with epoxides.

A. Morena,[a,b] V. Campisciano,[b] A. Santiago-Portillo,[a] F. Giacalone,[b] M. Gruttadauria,[b] C. Aprile[a]

[a]*Unit of Nanomaterials Chemistry, Department of Chemistry, NISM, University of Namur, 61 rue de Bruxelles, 5000 Namur, Belgium*

[b]*Department of Biological, Chemical and Pharmaceutical Sciences and Technologies (STEBICEF)- University of Palermo and INSTM UdR – Palermo, Viale delle Scienze, Ed.17, Palermo I-90128, Italy*

Figure S1. Solid state CP-MAS TOSS ^{13}C NMR of **POSS_TSP_AlCl.**

Figure S2. XPS Survey (a) and N1s High resolution (b) of **POSS_TSP_AlCl.**

Figure S3. Pressure/Temperature vs. Time plot for Leaching test with the mixture of the reaction between styrene oxide and CO2, catalized by POSS_TSP_AlCl_imiBr**.**

Figure S4. ^1H NMR (400 MHz, DMSO) I cycle of Styrene oxide (Entry 1 Tab.1; Fig.6)

Figure S5. ^1H NMR (400 MHz, DMSO) III cycle of Styrene oxide (Fig.6).

Figure S6. ^1H NMR (400 MHz, DMSO) V cycle of Styrene oxide (Fig.6).

Figure S7. ^1H NMR (400 MHz, DMSO) Glycidol (Entry 2 Tab.1)

Figure S8. ^1H NMR (400 MHz, DMSO) Epichlorohydrine (Entry 5 Tab.1)

Figure S9. ^1H NMR (400 MHz, DMSO) Epichlorohydrine (Entry 6 Tab.1)

Figure S10. ^1H NMR (400 MHz, DMSO) Cyclohexene oxide (Entry 9 Tab.1)

Figure S11. a) Pressure variation during the reaction time of the reaction between Epichlorohydrin and CO_2 at 100 °C for 3h and without any pressure refill. (Entry 5; Tab. 1) b) Pressure variation during the reaction time of the reaction between Epichlorohydrin and CO_2 at 100 °C for 3h and with a pressure refill after 1h. (Entry 6; Tab. 1)

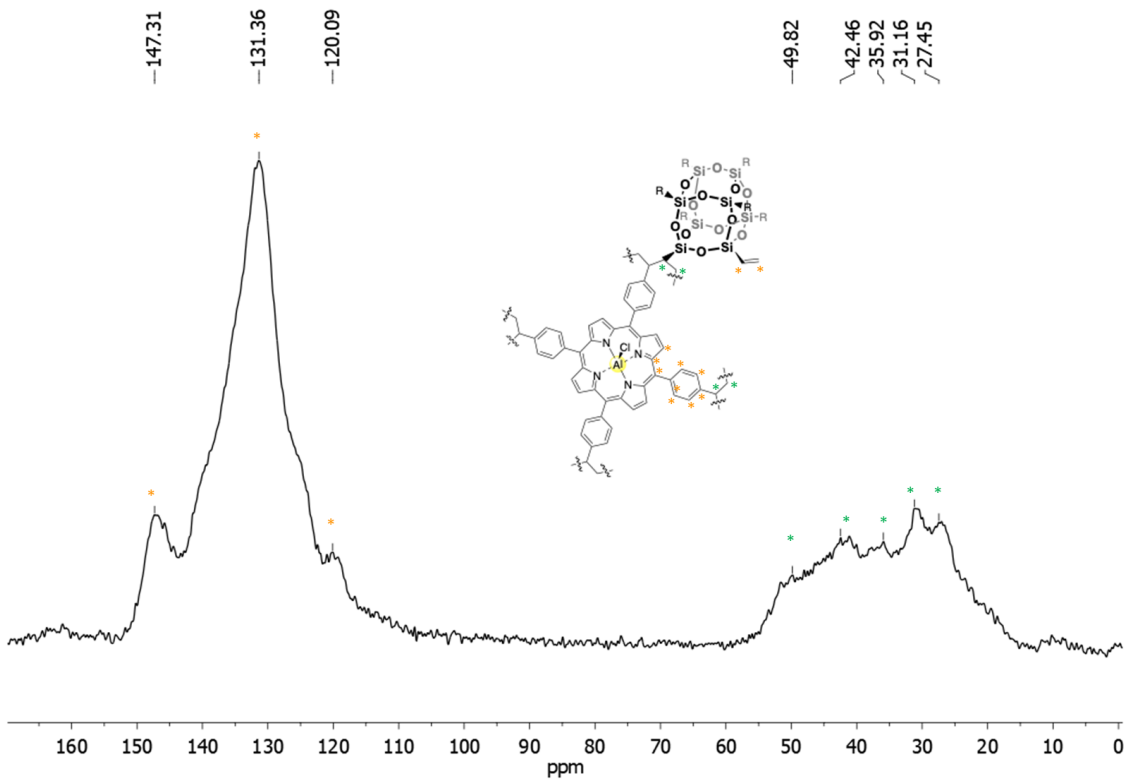

Figure S1. Solid state CP-MAS TOSS ^{13}C NMR of **POSS_TSP_AlCl.**

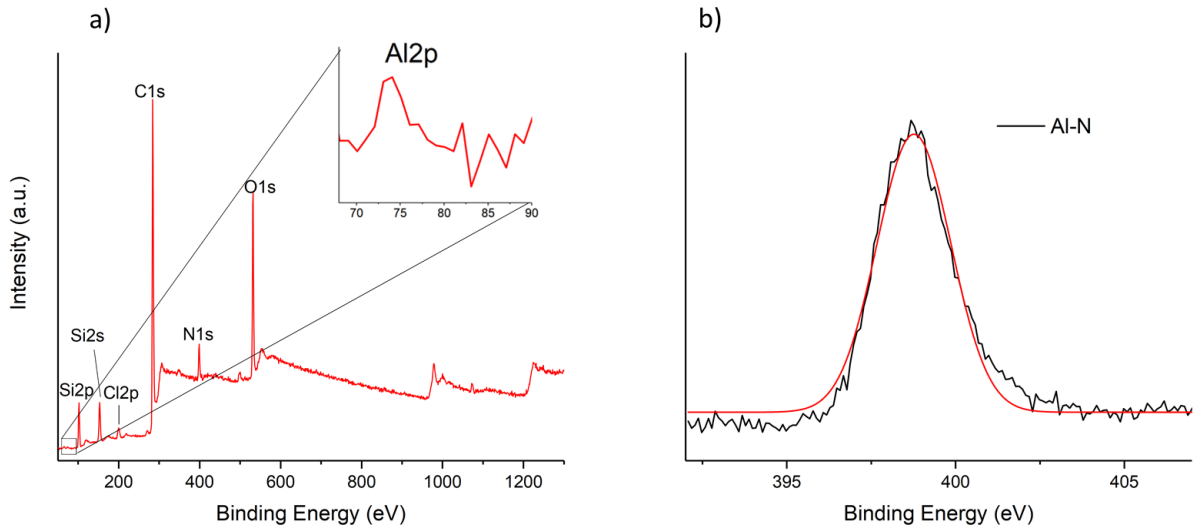

Figure S2. XPS Survey (a) and N1s High resolution (b) of **POSS_TSP_AlCl.**

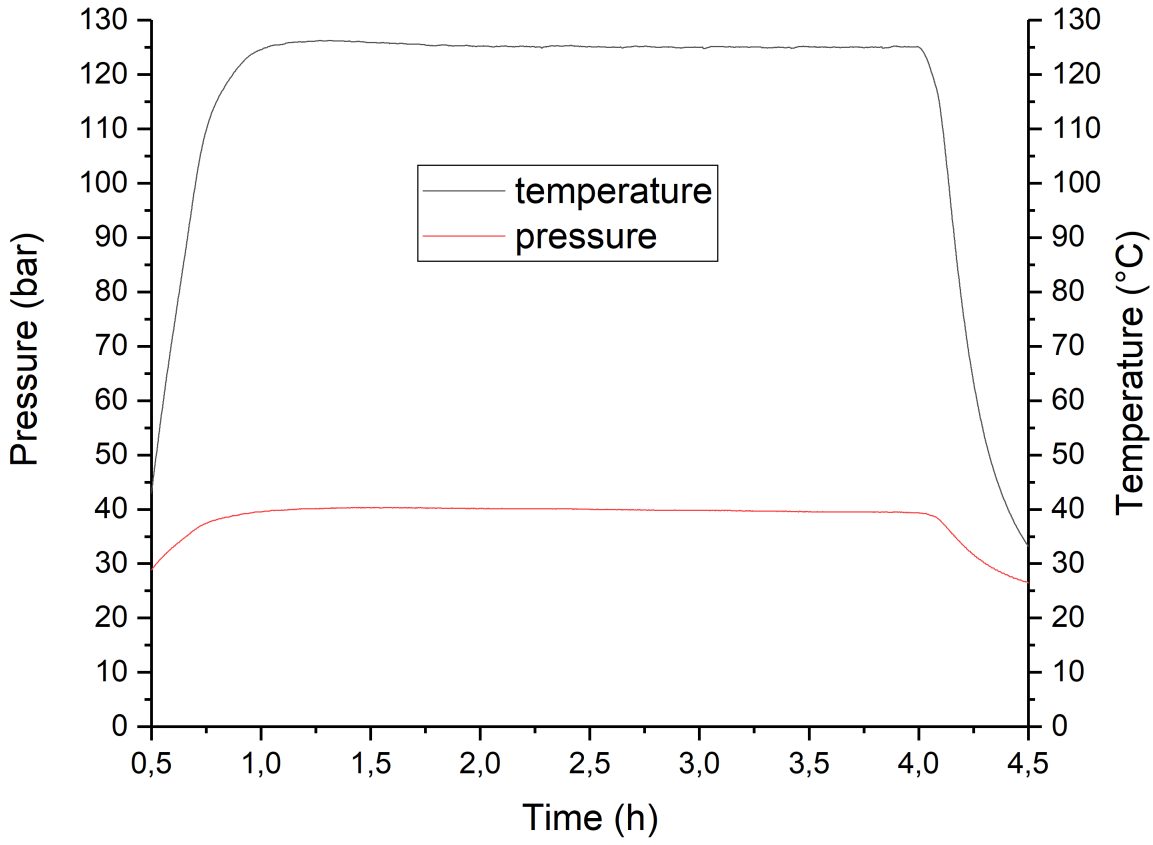

Figure S3. Pressure/Temperature vs. Time plot for Leaching test with the mixture of the reaction between styrene oxide and CO2, catalized by POSS_TSP_AlCl_imiBr**.**

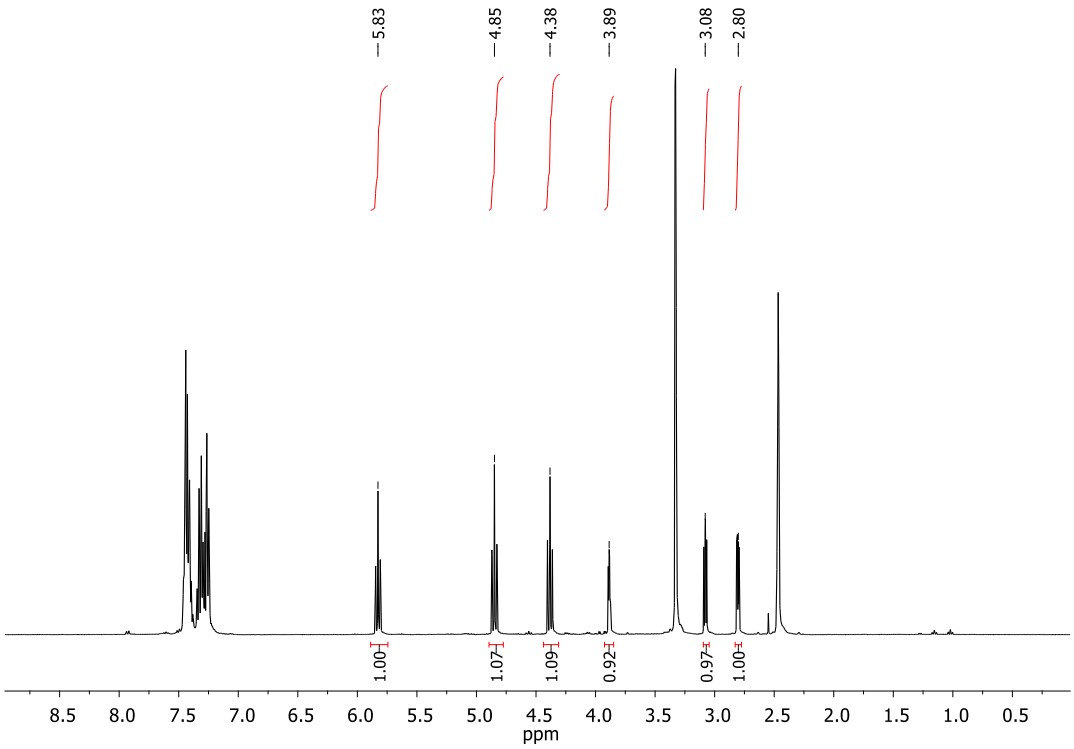

Figure S4. ^{1}H NMR (400 MHz, DMSO) of the reaction mixture I cycle Entry 1 Table 1; (Fig.6)

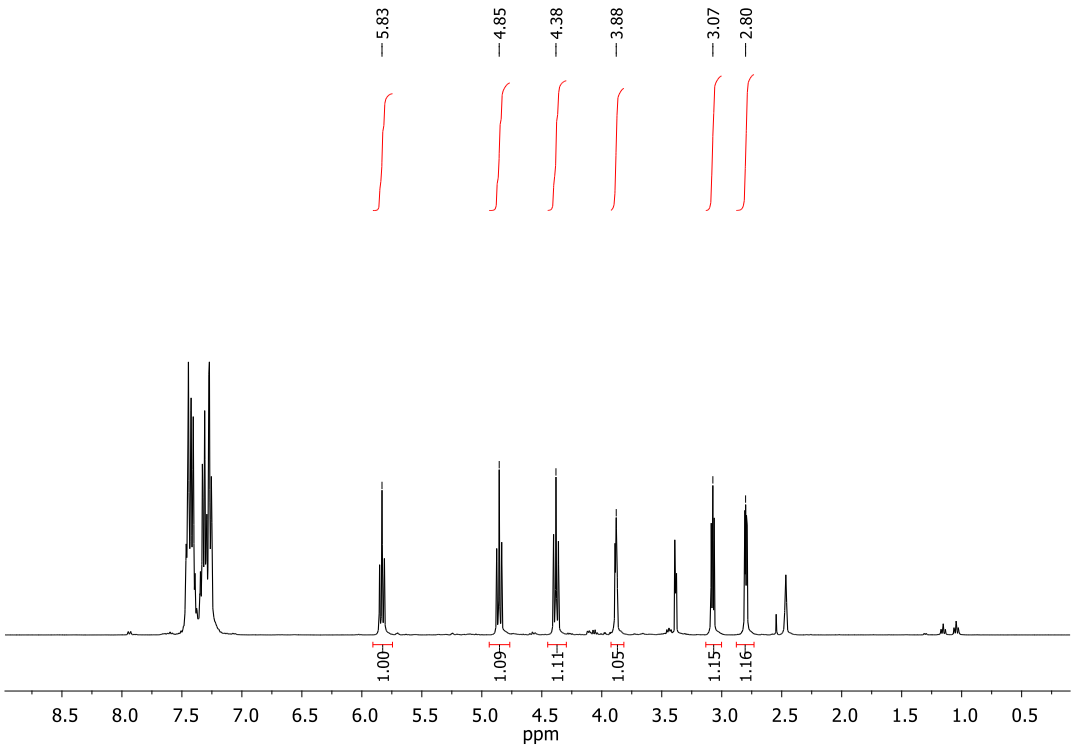

Figure S5. ^{1}H NMR (400 MHz, DMSO) of the reaction mixture III cycle, Fig.6.

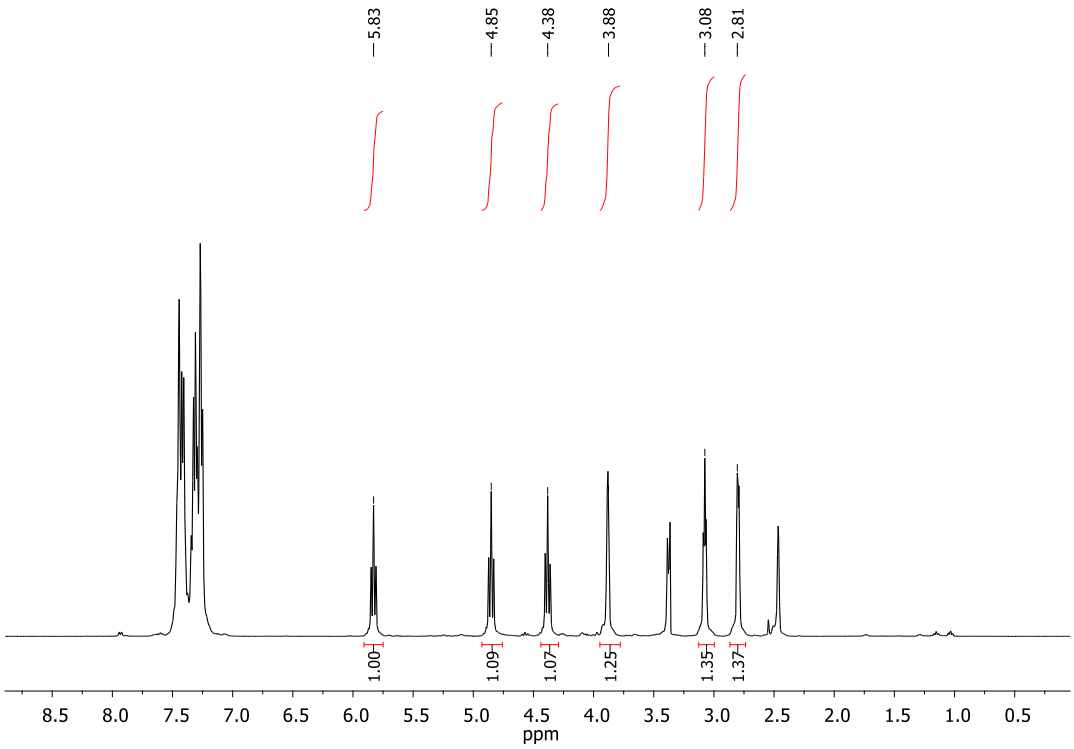

Figure S6. [1]H NMR (400 MHz, DMSO) of the reaction mixture V cycle, Fig.6.

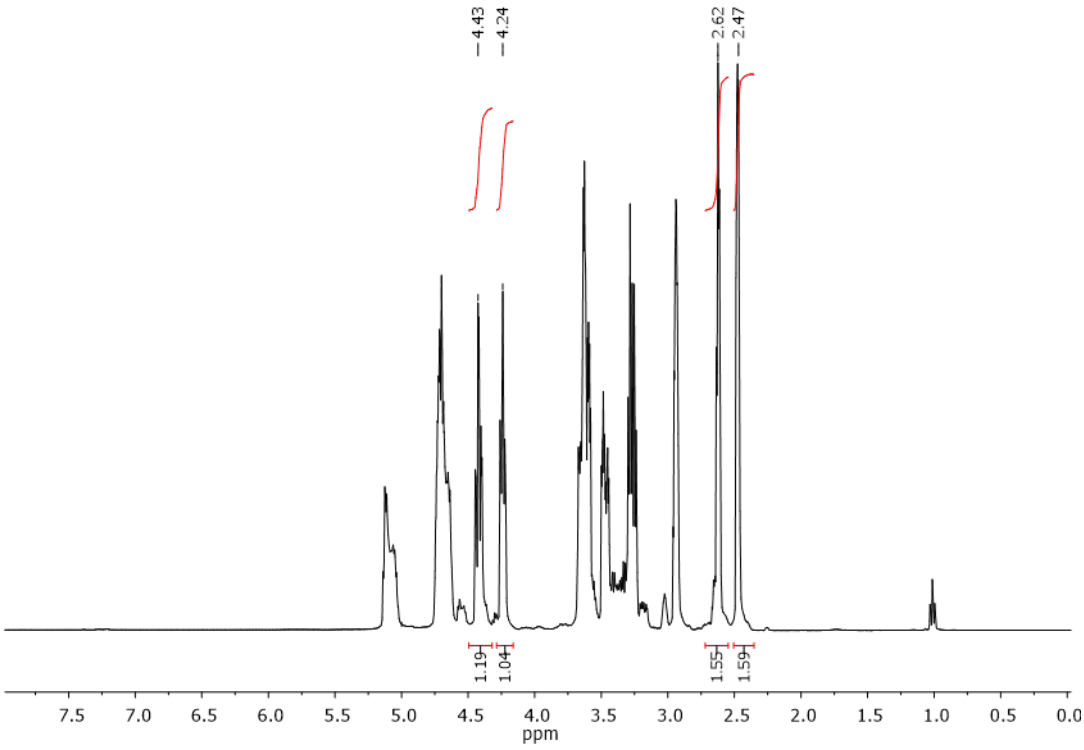

Figure S7. [1]H NMR (400 MHz, DMSO) of the reaction mixture Entry 2, Table 1

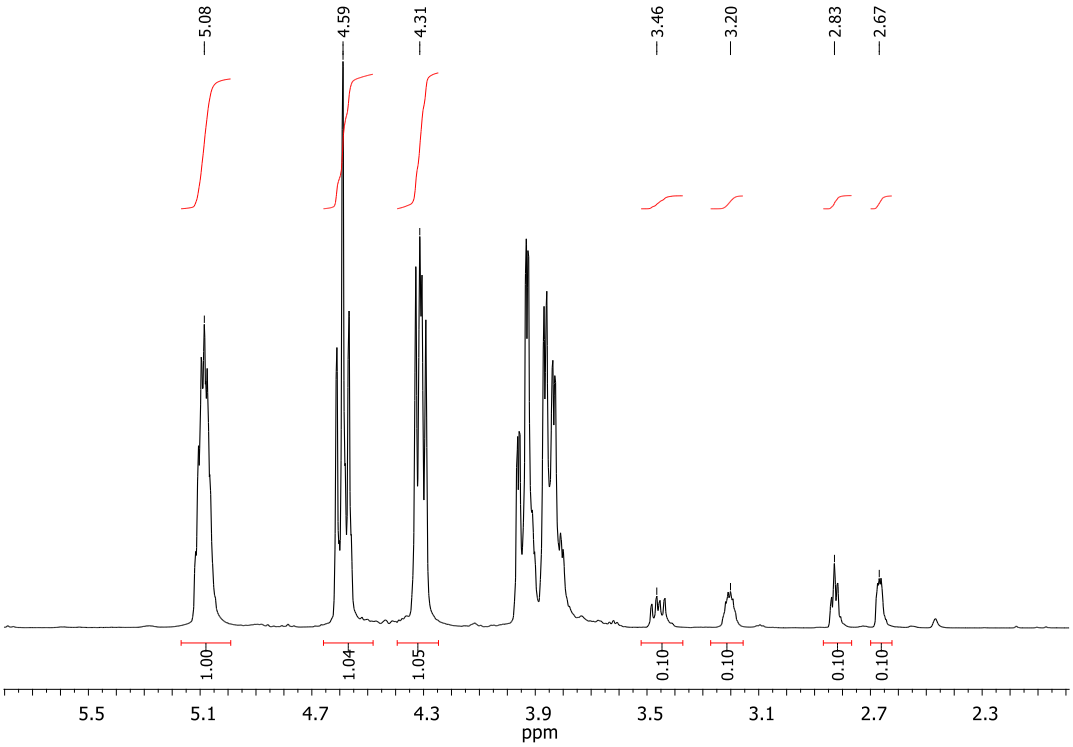

Figure S8. ^{1}H NMR (400 MHz, DMSO) of the reaction mixture Entry 5, Table 1

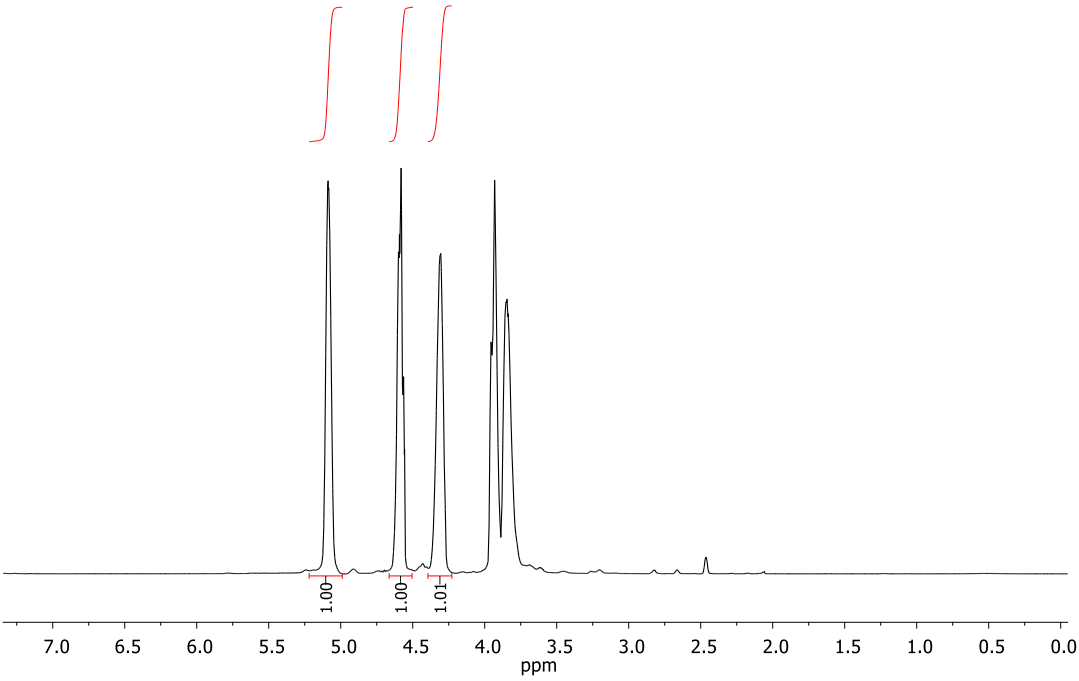

Figure S9. ^{1}H NMR (400 MHz, DMSO) of the reaction mixture Entry 6, Table 1

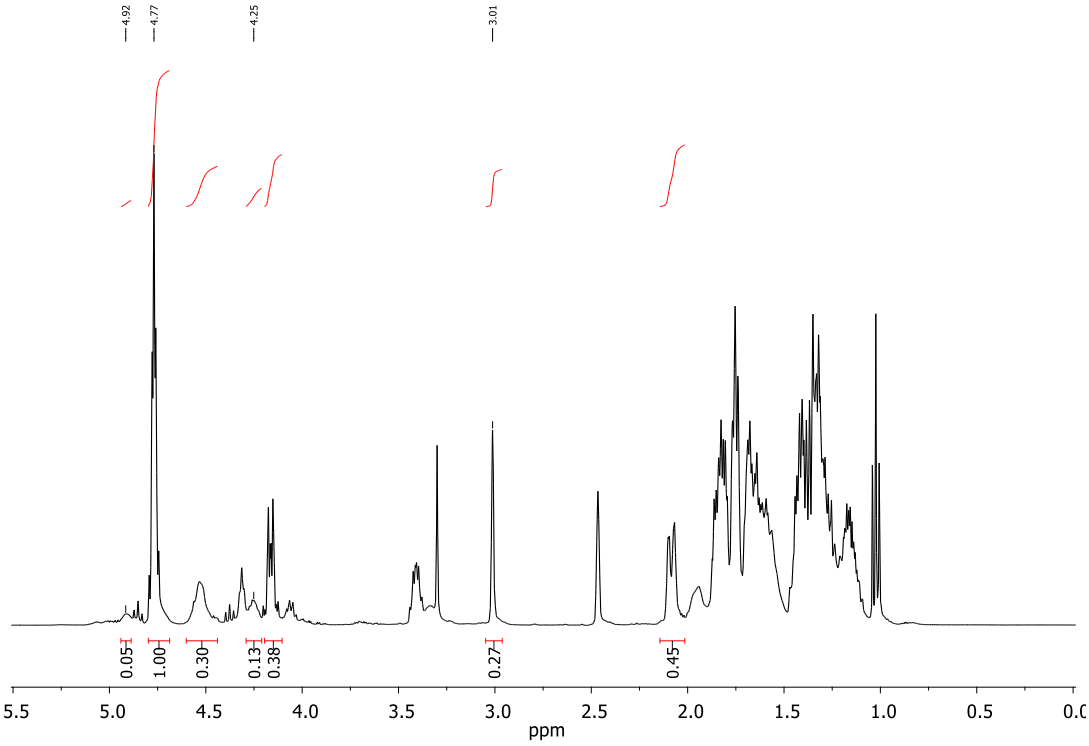

Figure S10. ^{1}H NMR (400 MHz, DMSO) of the reaction mixture Entry 9, Table 1

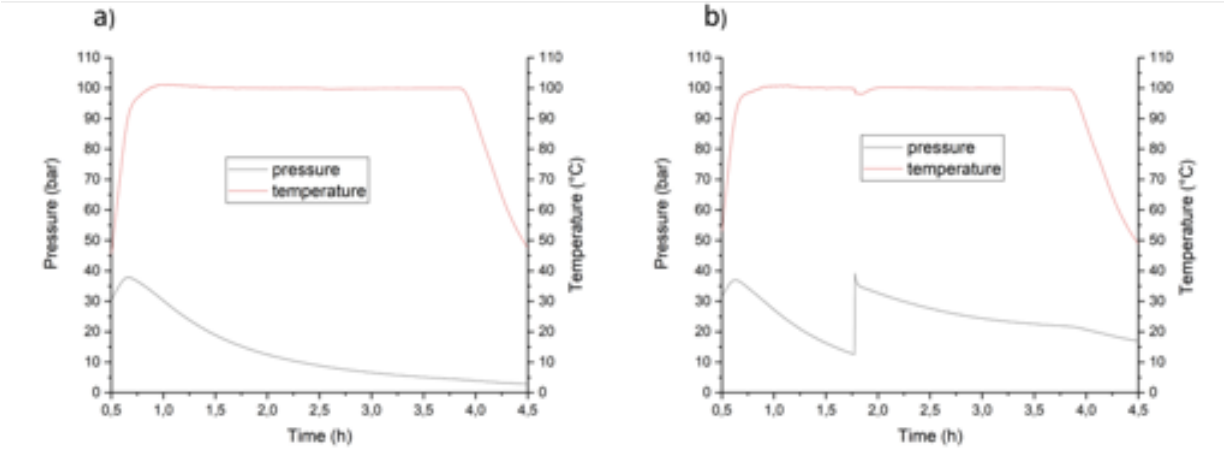

Figure S11. a) Pressure variation during the reaction time of the reaction between epichlorohydrin and CO_2 at 100 °C for 3h and without any pressure refill. (Entry 5; Tab. 1) b) Pressure variation during the reaction time of the reaction between epichlorohydrin and CO_2 at 100 °C for 3h and with a pressure refill after 1h. (Entry 6; Tab. 1)